Optics Letters

Fresnel lens optical fiber tweezers to evaluate the vitality of single algae cells

Asa Asadollahbaik,[1,2] Aashutosh Kumar,[3] Michael Heymann,[2] Harald Giessen,[1] and Jochen Fick[3,*]

[1]4th Physics Institute and Research Center SCoPE, University of Stuttgart, Pfaffenwaldring 57, 70569 Stuttgart, Germany
[2]IBBS, University of Stuttgart, Pfaffenwaldring 57, Stuttgart, 70569, Germany
[3]Université Grenoble Alpes, CNRS, Institut Néel, 38000 Grenoble, France
*Corresponding author: jochen.fick@neel.cnrs.fr

Received 3 November 2021; revised 24 November 2021; accepted 26 November 2021; posted 29 November 2021; published 23 December 2021

Dunaliella salina **algae are trapped and studied using dual-fiber optical tweezers based on nano-imprinted Fresnel lenses. Different forms of cyclic motion of living algae inside the optical trap are observed and analyzed. A characteristic periodic motion in the 0–35 Hz frequency region reflects the algal flagella activity and is used to estimate the algal vitality, by photomovement. The trap stiffness and optical forces are measured for the case of a dead algal cell. It is shown that the dual-fiber optical tweezers can be used to study the vitality (or viability) property of single cells, a property that is essential and can be scaled up to other applications, such as sperm analysis for fertility tests.**

https://doi.org/10.1364/OL.447683

Optical tweezers have become a standard tool in many interdisciplinary research domains owing to the possibility of trapping, manipulating, sorting, and separating micrometer- and nanometer-sized objects [1,2]. Most of the ongoing research is based on the original approach of using a high numerical aperture microscope objective to focus the laser beam for trapping [3]. In 1993, the first optical fiber-based optical tweezers were demonstrated by aligning two fiber pigtailed lasers using just a cover slip and a capillary [4]. This first realization highlights the outstanding simplicity and the small footprint of optical fiber tweezers. Today, microstructured optical fibers allow the development of a great variety of optical tweezers with different properties and many applications from nanophysics to biology [5–11]. We have also used two different types of microstructured fiber tweezers, one with sharp-tipped fibers and another with Fresnel lens-tip fibers, for dual-fiber trapping of synthetic particles and have shown a variety of pros and cons for either arrangement [5,6,12]. The dual-fiber optical tweezers based on a Fresnel lens have the advantage of high trapping efficiency at very low laser powers. This is a great advantage for trapping and manipulation of biological cells. At the same time, the ease and simplicity of the development and fabrication process of these fibers are of great advantage in comparison with other miniaturized dual-beam optical tweezers [13,14]. As an example, Yu *et al.* [13] have developed on-chip dual-beam optical tweezers, producing out-of-plane trapping. This work requires several stages of microfabrication, including lithography and metal deposition. Such processes are complicated and expensive and thus limit the possible applications. Ti *et al.* [14] also developed another on-chip design using inclined fibers to provide out-of-plane trapping. This design involves using diverging beams and the results clearly show that the trapping efficiency and lower laser power required for trapping is not comparable to our Fresnel lens dual-fiber optical tweezers. Another advantage of Fresnel lens dual-fiber optical tweezers is the fact that they can be combined with microfluidic channels and produce in-plane trapping.

In the field of biology, optical tweezers are used to manipulate different natural entities, to trap subcellular compartments in plants [15] and animals [16], to study mechanical properties of blood cells [17–19], to trap and manipulate different species of algae, including a variety of biflagellated algae cells, or study their rotational behavior and observe their deflagellation (the process of losing their flagella) owing to photostimulus [20–22]. In this work, we use our dual-fiber Fresnel lens optical tweezers to trap and manipulate a specific biflagellated algae, known as *Dunaliella salina*. The study of photomovement of these algae is particularly interesting as it is the basis of fundamental biological processes, such as photosynthesis, energy transformation, and membrane-mediated phenomena in these cells [23,24]. We study the behavior of the cell in the optical trap in response to immobilization and different laser powers until deflagellation and demonstrate the correlation between flagella and cell vitality.

Our optical fiber tweezers are depicted in Fig. 1(a). An 808 nm trapping laser (LU0808M250, Lumics) is separated into two equal arms using a polarizing beam splitter and a half-wave plate to control the relative light power in each arm. The light beam is coupled to the optical fibers using fiber launchers. Before and after each experiment, the output powers of the two identical Fresnel fibers are measured in air. The given power values correspond to the emitted power of one fiber in air. The fibers are mounted on two sets of *xyz* piezoelectric translation stages for high precision position alignment (PI P-620 and SmarAct SLC-17 series). The trapping chamber consists of an O-ring placed in between two glass slides and cut in two parts in order

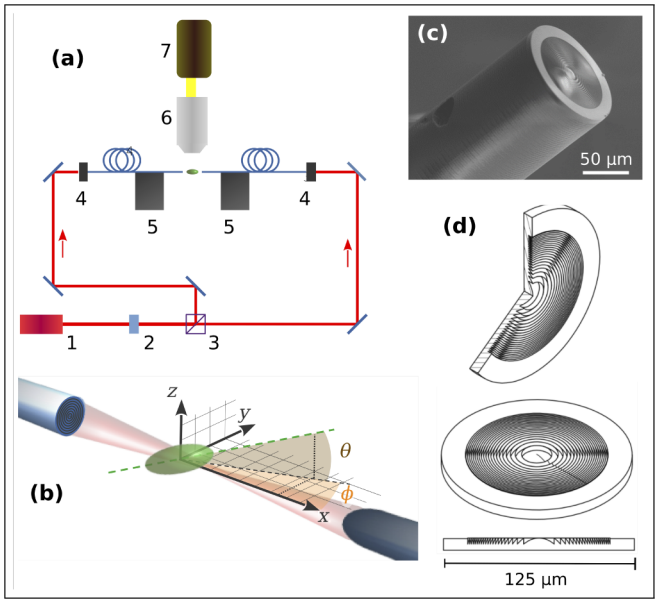

Fig. 1. (a) Experimental optical trapping setup (1: 808 nm laser; 2: $\lambda/2$ wave plate; 3: polarizing beam splitter; 4: fiber launchers; 5: *xyz* piezo-stages; 6: 50× long working distance objective; 7: CMOS camera). (b) Arrangement (not to scale) of trapped alga (green) in between the two Fresnel fibers and definition of polar angle θ and azimuth angle ϕ. (c) and (d) Scanning electron micrograph and sketch of Fresnel lens fiber with NA = 0.5 and a working distance of 100 µm.

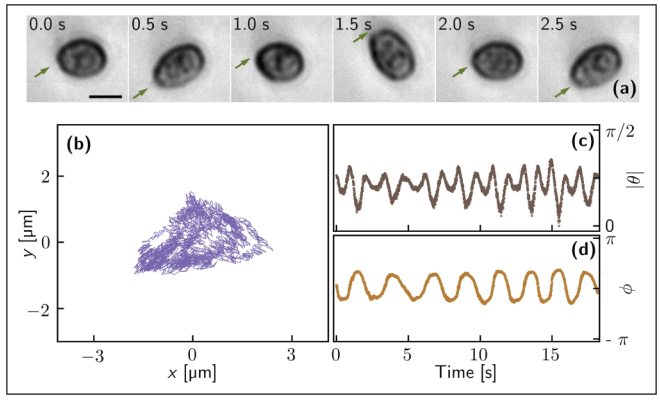

Fig. 2. Optical trapping of living alga at P_{opt} = 4.8 mW (see Visualization 1). (a) Time sequence (scale bar, 5 µm; arrows indicate flagellal position). (b) Position tracking plot of the trapped alga. (c) Time-dependent polar angle $|\theta|$. (d) Time-dependent azimuth angle ϕ.

to insert the fibers. All experiments are carried out at room temperature. A homemade microscope, consisting of a long working distance microscope objective (Mitutoyo G Plan Apo 50x) and a CMOS camera (Hamamatsu ORCA FLASH 4.0 LT), is used for the observation of trapping incidents. Typical trapping videos contain 4000 frames recorded at frame rates of 220 frames per second (fps). The time-dependent alga position and orientation are obtained by means of a custom Python script. For each video frame, the image of the alga is fitted to a 2D ellipse. Its center is takes as the alga position. The orientation of the ellipse long axis a defines the azimuth angle ϕ. The absolute value of the polar angle $|\theta|$ is calculated using $\sin(|\theta|) = a/a_{ell}$, with $2 \cdot a_{ell}$ being the algal size [Fig. 1(b)].

The Fresnel lenses are printed on standard, commercial single-mode fibers (Nufern 780-HP) by femtosecond two-photon lithography (Nanoscribe Photonic Professional GT) with commercial resist (Nanoscribe IP-Dip) [12,25]. The total writing time is 55 min. To achieve a reasonable working distance at high numerical aperture, the optical fiber mode is expanded by propagation through a solid cylinder of 500 µm length. The chosen Fresnel lens fibers, with NA = 0.5, produce a tightly focused Gaussian spot with a waist of 0.8 µm at a focal distance of f = 97.5 µm in water.

Living cells of *Dunaliella salina*, a photosynthetic biflagellated alga with high motility, approximately 9×6 µm^2 in size, are chosen for optical trapping experiments. Prior to trapping experiments, all cells are transferred into a combination of their lake water and deionized water until an adequate cell density is reached. The algae are efficiently trapped at optical powers of typically 4–5 mW. These algae are of ellipsoidal shape and have a soft membrane; some of the cell's internal structure is visible in the videos. However, no deformation of the alga shape is observed during trapping. In the present case of living algae, the main force to be overcome by the optical trap potential is not Brownian motion, but the active algal agitation. Thus, the minimal trapping light intensity depends on the algal vitality. As can be seen in Visualization 1 and Visualization 2, the alga attempts to escape the optical tweezers by fast movement of its flagella. This action results in rotation of the trapped alga inside a trapping region of typically 6×4 µm^2, approximately the same order as the alga size.

In the first video, the laser power (trapping power) is fixed at P_{opt} = 4.8 mW (Fig. 2). The alga is mainly rotating around the optical axis with a conical trajectory. The corresponding oscillation around the azimuth angle is at 0.45 Hz frequency, with a cone angle of $\theta^{max} \approx 50°$. It can be observed that the turning tail of the alga is the one with the flagella and that the opposite tail is stationary.

A different behavior is observed in the same trapping incident but at slightly lower optical power of P_{opt} = 3.8 mW (Fig. 3). Here, the alga is mainly turning in the observation plain in the anticlockwise direction with a frequency of about 0.39 Hz. This rotation is accompanied by a less frequent reversal rotation perpendicular to the observation plane. In other words, the alga is mostly rotating around its center and not around the distal end to the flagella, as in the previous video. Moreover, the algal position range in the trap becomes greater and more anisotropic, to the extent of 7.5×2.3 µm^2.

After two more trapping videos (not presented here), the alga's behavior changes, and a significant reduction in its vitality is observed. Its movement in the optical trap changes drastically (Fig. 4) and it remains trapped at a low laser power of only P_{opt} = 1.1 mW. One can conclude that the alga died. Comparing the position tracking plots for the dead alga [Fig. 4(a)] with the one for the living alga (Figs. 2 and 3), the position range of the dead alga is much smaller. Moreover the angular oscillations have totally disappeared and the alga remains aligned with its long axis parallel to the axis of the laser beam. Finally, when switching off the trapping laser, the dead algae slowly drifts out of the trap. This observation is in clear contrast with the active cell motion with speeds of the order of 3–4 µm·s^{-1} (Fig. 5, inset).

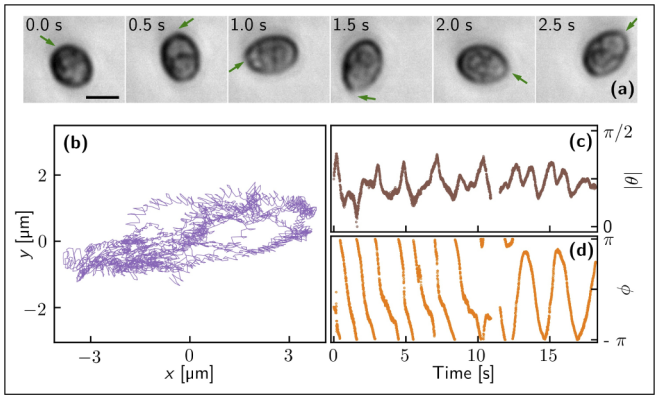

Fig. 3. Optical trapping of the same living alga as in Fig. 2 at P_{opt} = 3.8 mW (see Visualization 2). (a) Time sequence (scale bar, 5 µm; arrows indicate the flagella position). (b) Position tracking plot. (c) Time-dependent polar angle $|\theta|$. (d) Time-dependent azimuth angle ϕ.

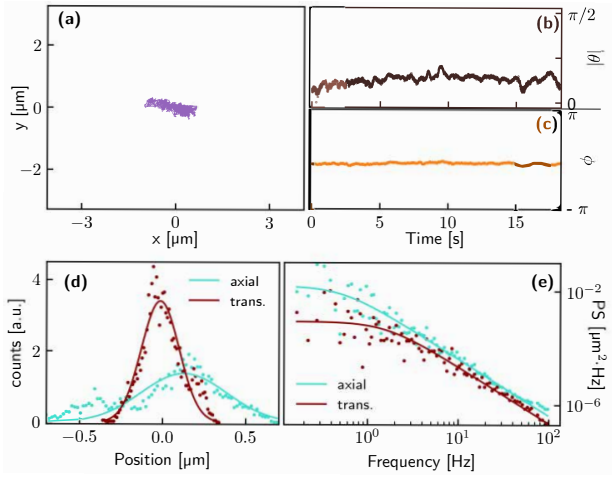

Fig. 4. Trapping of the dead alga (same alga as Figs. 2 and 3) at P_{opt} = 1.1 mW. (a) Position tracking record. (b) Time-dependent polar angle $|\theta|$. (c) Time-dependent azimuth angle ϕ. (d) Boltzmann statistics. (e) Power spectrum analysis of the trapping incident for axial and transverse directions relative to the fiber axis.

In the case of a dead alga, which can be considered as a passive object, it is possible to determine the trap stiffness κ by applying Boltzmann statistics (BS) and power spectrum analysis (PSA) [Figs. 4(d) and 4(e)], as described in Ref. [5]. The position distribution in the transverse direction follows a Gaussian shape, thus allowing us to determine κ with good precision. In the axial direction, the two sub-peaks are, however, approximated by only one Gaussian in order to get an approximation of the trap efficiency. In the case of PSA, the experimental data are well fitted by the Lorentz function of the harmonic oscillator model. However, at low frequencies, the dispersion of the experimental points is high. Moreover, the fact that the algal surface is not smooth is not included in the calculation of the Stokes friction coefficient. The trapping stiffness in the axial direction is calculated to be 123 fN·µm^{-1} and 100 fN·µm^{-1} using BS and PSA, respectively. The transverse trapping stiffness is similarly calculated and has a value of 318 fN·µm^{-1} using BS analysis, and

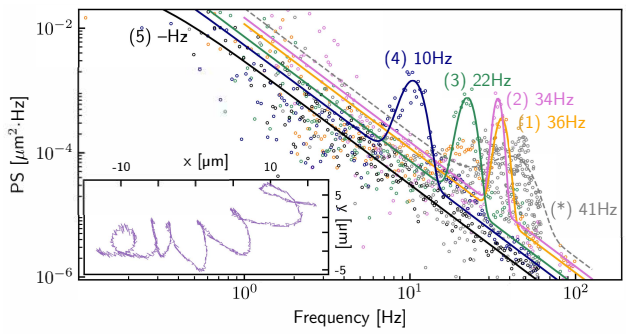

Fig. 5. Power spectra (total motion in the *xy* plane) for five videos, recorded successively on the same alga: (1), (2), and (5) correspond to the videos presented in Figs. 2, 3, and 4, respectively. For comparison, the result of an untrapped cell is added (*) and its position tracking record (over 6 s) is displayed in the inset. The solid lines are numerical fits to estimate the indicated oscillation frequencies.

310 fN·µm^{-1} using PSA. Despite the exposed limits, the respective values obtained by PSA and BS are of the same order. The main result is that the trapping efficiency in the transverse direction is about three times higher than that in the axial direction. This feature, which is currently observed for dual-beam optical tweezers, results from the trap anisotropy. In the axial direction, the repulsive scattering forces of the two beams cancel each other in the trap center, whereas in the transverse direction the gradient forces of both beams attract the object to the beam center [5,12].

All the results presented so far are extracted from different videos of one single optical trapping experiment with the same alga. The only varying parameters are the applied optical trapping power and the total time the alga was already trapped. For each video presented in Figs. 2 to 4, the alga is either alive and agile and shows a high vitality, or it is dead. The question is whether this transition is abrupt or slow and how to identify it. In Figs. 2(a) and 3(a), fast loops in the position tracking records are observed. These oscillations at a well defined and specific frequency result in a characteristic peak in the power spectra (Fig. 5). In this series of five videos, successively recorded in a 30 min time period, the peak frequency decreases steadily from 36 Hz to 10 Hz before vanishing in the last video (Fig. 4). The origin of this fast motion is the attempt of the alga to escape the optical trap, using its flagella. The frequency can thus be related to the alga's flagellal oscillations. With increasing trapping time, the alga loses energy and becomes enervated before dying by exhaustion. These fast loops in the position records can thus be used as an indicator for the alga's vitality level. A similar behavior is observed with an untrapped living cell (Fig. 5 inset and gray curve). The oscillation frequency is less well defined, but still clearly visible. At 41 Hz, the oscillation frequency is slightly above the frequencies of the trapped alga.

The optical forces operating in our dual-beam optical tweezers are directly measured by blocking one of the two trapping beams (Fig. 6). For example, when blocking the beam of the left Fresnel lens fiber, the alga is pushed to the left side by the optical forces of the beam coming from the fiber on the right-hand side. Owing to its asymmetric shape, the alga slowly rotates during this movement, thus explaining its nonlinear trajectory. Under this experimental condition, the algal speed is proportional to the optical force as $F^{opt} = \gamma_0 \cdot v$, with $\gamma_0 = 6\pi\eta a$ the Stokes friction

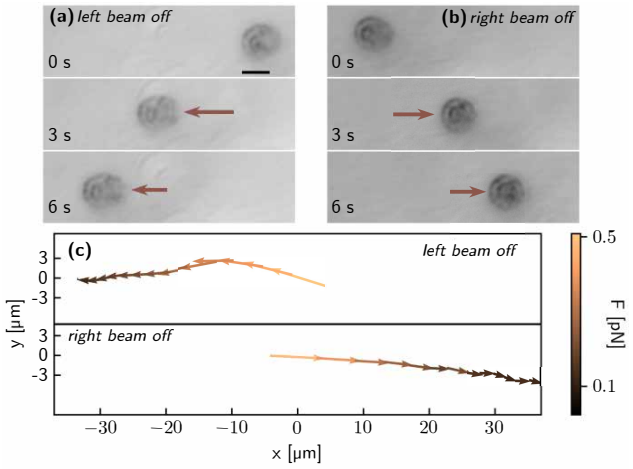

Fig. 6. Optical force measuring experiment. (a) and (b) Time sequence of alga pushed to (a) the left and (b) the right by blocking of the opposite laser beam. At $t = 0$ s, both beams are on and the alga is stably trapped at $x = 0$. The arrows are a guide to underline the algal motion. (c) Calculated optical forces at $P_{opt} = 13.6$ mW. The arrows' colors and lengths are proportional to the force magnitude.

coefficient, a the alga radius, and η the dynamic viscosity of water [5]. The measured optical force shows a maximum at the trapping spot, with absolute values of 479 fN and 462 fN when the alga is pushed by the right and left beams, respectively. In the vicinity of the trapping spot, the force is linearly decreasing with distance with slopes of $-11\,\mathrm{fN}\cdot\mu\mathrm{m}^{-1}$ and $14\,\mathrm{fN}\cdot\mu\mathrm{m}^{-1}$, respectively.

In conclusion, efficient optical trapping of living and motile *Dunaliella salina* algae is realized for light powers of 4–5 mW. The living alga tries to escape the trap but is confined to a volume of the order of its size. Its flagellal action results in a regular and cyclic motion inside the trap. The periodic oscillations of the alga's position can be used as a measure of its vitality. After some time, the alga gets exhausted and the dead cell can be trapped at lower laser powers of about 1 mW and mean trap stiffnesses of ≈ 100 and $\approx 300\,\mathrm{fN}\cdot\mu\mathrm{m}^{-1}$ in the axial and transverse directions, respectively. Moreover, the optical force of each trapping beam is estimated at 0.5 pN. Our results show that our approach is efficient for trapping of living entities, such as algae. The possibility to constrain them inside a small volume will allow for an in-depth study of the alga properties, e.g., their vitality as a function of environmental parameters. In this context, the use of Fresnel lens fibers with large working distances allows trapping at a large distance from the fibers and thus removes any influence from the fibers on the movement of the alga. Considering the similar values of the motility of algae and sperm, one can also envision that this methodology can be expanded to study the viability of sperm cells, an important parameter in fertility tests.

Funding. Agence Nationale de la Recherche (Spectra ANR-16-CE24-0014-01); European Research Council (PoC 3D PrintedOptics, Nr.86254); Deutsche Forschungsgemeinschaft (GRK 262); Bundesministerium für Bildung und Forschung (Printoptics); Ministerium für Wissenschaft, Forschung und Kunst Baden-Württemberg (ICM); Terra Incognita; BW Stiftung (Opterial).

Acknowledgment. We thank Ms Tatjana Kleinow from the IBBS molecular biology core facility for her support and assistance in providing *Dunaliella salina* samples.

Disclosures. The authors declare no conflicts of interest.

Data availability. Data underlying the results presented in this paper are not publicly available at this time but may be obtained from the authors upon reasonable request.

REFERENCES

1. S. E. S. Spesyvtseva and K. Dholakia, ACS Photonics **3**, 719 (2016).
2. G. Pesce, P. H. Jones, O. M. Maragó, and G. Volpe, Eur. Phys. J. Plus **135**, 949 (2020).
3. A. Ashkin, J. M. Dziedzic, J. E. Bjorkholm, and S. Chu, Opt. Lett. **11**, 288 (1986).
4. A. Constable, J. Kim, J. Mervis, F. Zarinetchi, and M. Prentiss, Opt. Lett. **18**, 1867 (1993).
5. J.-B. Decombe, S. Huant, and J. Fick, Opt. Express **21**, 30521 (2013).
6. G. Leménager, K. Lahlil, T. Gacoin, G. C. des Francs, and J. Fick, J. Nanophotonics **13**, 012505 (2018).
7. J. S. Paiva, P. A. Jorge, C. C. Rosa, and J. P. Cunha, Biochim. Biophys. Acta, Gen. Subj. **1862**, 1209 (2018).
8. H. Lee, J. Park, and K. Oh, J. Lightwave Technol. **37**, 2590 (2019).
9. X. Zhao, N. Zhao, Y. Shi, H. Xin, and B. Li, Micromachines **11**, 114 (2020).
10. A. Kumar, J. Kim, K. Lahlil, G. Julie, S. N. Chormaic, J. Kim, T. Gacoin, and J. Fick, J. Phys. Photonics **2**, 025007 (2020).
11. Q. Zhao, H.-W. Wang, P.-P. Yu, S.-H. Zhang, J.-H. Zhou, Y.-M. Li, and L. Gong, Front. Bioeng. Biotechnol. **8**, 422 (2020).
12. A. Asadollahbaik, S. Thiele, K. Weber, A. Kumar, J. Drozella, F. Sterl, A. Herkommer, H. Giessen, and J. Fick, ACS Photonics **7**, 88 (2020).
13. S. Yu, J. Lu, V. Ginis, S. Kheifets, S. W. D. Lim, M. Qiu, T. Gu, J. Hu, and F. Capasso, Optica **8**, 409 (2021).
14. C. Ti, Y. Shen, M.-T. H. Thanh, Q. Wen, and Y. Liu, Sci. Rep. **10**, 20099 (2020).
15. T. Ketelaar, N. de Ruijter, and S. Niehren, in *Plant Cell Morphogenesis* (Springer, 2019), pp. 231–238.
16. I. A. Favre-Bulle, A. B. Stilgoe, E. K. Scott, and H. Rubinsztein-Dunlop, Nanophotonics **8**, 1023 (2019).
17. J. Guck, R. Ananthakrishnan, T. J. Moon, C. Cunningham, and J. Käs, Phys. Rev. Lett. **84**, 5451 (2000).
18. J. Guck, R. Ananthakrishnan, H. Mahmood, T. J. Moon, C. C. Cunningham, and J. Käs, Biophys. J. **81**, 767 (2001).
19. J. Guck, S. Schinkinger, B. Lincoln, F. Wottawah, S. Ebert, M. Romeyke, D. Lenz, H. M. Erickson, R. Ananthakrishnan, D. Mitchell, J. Käs, S. Ulvick, and C. Bilby, Biophys. J. **88**, 3689 (2005).
20. B. A. Juarez, V. G. Garces, B. Cordero-Esquivel, G. C. Spalding, and K. A. O'Donnell, Sensors **20**, 5656 (2020).
21. M. Gudipati, J. S. D'Souza, J. A. Dharmadhikari, A. K. Dharmadhikari, B. J. Rao, and D. Mathur, Opt. Express **13**, 1555 (2005).
22. V. G. Garces, O. Salazar-Oropeza, B. Cordero-Esquivel, and K. A. O'Donnell, Appl. Opt. **54**, 1827 (2015).
23. N. Masyuk, Y. I. Posudin, and G. Lilitskaya, Int. J. Algae **7**, 310 (2005).
24. Y. I. Posudin, N. P. Massjuk, and G. G. Lilitskaya, *Photomovement of Dunaliella Teod* (Springer, 2010).
25. T. Gissibl, S. Wagner, J. Sykora, M. Schmid, and H. Giessen, Opt. Mater. Express **7**, 2293 (2017).